Electronic Supplementary Information

Coordination environment evolution of Co (II) during dehydration and re-crystallization processes of $KCoPO_4 \cdot H_2O$ towards enhanced electrocatalytic oxygen evolution reaction

Quande Che,*[a] Xiaobin Xie,[b] Qian Ma,[a] Junpeng Wang,[a] Yuanna Zhu,[a] Ruixia Shi,[a] Ping Yang*[a]

[a] School of Materials Science and Engineering, University of Jinan, Jinan 250022, P. R. China.

E-mail: mse_cheqd@ujn.edu.cn, mse_yangp@ujn.edu.cn

Tel.: +86 531 89736225; fax: +86 531 87974453

[b] School of Materials Science and Engineering, Wuhan University of Technology, Wuhan 430070, P. R. China.

1. Experimental

1.1 Materials

All reagents were used without further purification. Cobalt chloride ($CoCl_2 \cdot 6H_2O$, 98%), dipotassium hydrogenphosphate (K_2HPO_4, ≥98.0%), potassium hydroxide (KOH, ≥85.0 wt%) were purchased from Sinopharm Chemical Reagent Co. Ltd. Nafion solution (10 wt%) was purchased from Sigma-Aldrich Co. LLC. The DI water (resistance of 18.2 MΩ cm/ 25 °C) used in experiments was obtained from the Milli-Q system.

1.2 Characterization

Morphology and crystal structure studies were performed on the as-prepared $KCoPO_4 \cdot H_2O$ and $KCoPO_4$ samples using a field-emission scanning electron microscope (SEM, FEI, Quanta 250, the United States), X-ray diffraction

(XRD, D8 Advance Bruker), transimission electron microscope (TEM, Tecnai G2 F20, FEI), X-ray photoelectron spectroscopy (XPS, Thermo Scientific ESCALab 250Xi), and TGA thermogravimetric simultaneous thermal analyzer (STA8000).

1.3 Electrochemical measurements

All the electrocatalytic measurements were carried out on a PARSTAT4000+ electrochemical workstation in 1M KOH aqueous solution via a three-electrode configuration at room temperature. Catalyst powder was well dispersed in a mixture of isopropanol, water Nafion solution (10 wt%). Then, the ink was spread onto the surface of the glassy carbon electrode (mass loading: ~0.2 mg cm^{-2}) by a micropipette and dried under room temperature. The as-prepared $KCoPO_4 \cdot H_2O$ and $KCoPO_4$ were used as the working electrode. The Hg/HgO electrode and a platinum plate were used as the reference electrode and the counter electrode, respectively. The linear sweep voltammetry (LSV) measurements were carried out on a scan rate of 5 mV s^{-1}, with the iR compensation using the equation: $E_{iR\ corrected} = E - iR_s$, where R_s is the uncompensated ohmic solution resistance. Electrochemical impedance spectroscopy (EIS) tests were conducted with the frequency scan range from 10 kHz to 0.1Hz. Besides, all potentials in this research were reported versus the reversible hydrogen electrode (RHE), converted using the following equation:

$E_{RHE} = E_{Hg/HgO} + 0.098 + 0.059 \times pH$

where $E_{Hg/HgO}$ is the tested potential against the reference electrode.

In addition, the turnover frequency (TOF) was calculated according to the following equation[1]:

$$\mathrm{TOF} = \frac{j \times A}{4 \times F \times n}$$

where j is the current density obtained at overpotential of 400 mV in A cm^{-2}, A is the surface area of the electrode (0.0706 cm^2), F is the constant (96485.3 C mol^{-1}), and n is the moles of the catalyst loaded on the electrode.

2. Computational models and methods.

The computational calculations were performed with CASTEP module of the Materials Studio, [2] which is based on the density functional theory (DFT), [3, 4] with the Hubbard model (DFT + U). [5, 6] For a better description of the Co (3d) electrons, the effective U value of 3.3 eV was applied. A kinetic energy cut-off of 520 eV was used. The electronic wave function was expressed by the combination of plane wave basis, and the generalized gradient approximation (GGA) method with the Perdew-Burke-Ernzerhof (PBE) functional[7,8] was employed for exchange and correlation interactions. Ultrasoft pseudo potential was used to treated core electrons.[9] The Brillouin zones was performed by the Monkhorst-pack scheme sampled into 4 × 3 × 5 for $KCoPO_4 \cdot H_2O$ and 2 × 3 × 2 for $KCoPO_4$. The force and energy convergence criteria were set to 0.05 eV $Å^{-1}$ and 10^{-6} eV, respectively.

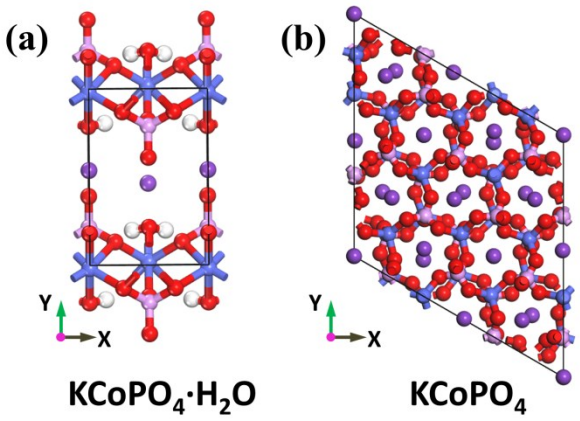

Fig. S1 Structural models of $KCoPO_4 \cdot H_2O$ and $KCoPO_4$. (Blue, red, pink, purple and white balls represent Co, O, P, K and H atoms, respectively.)

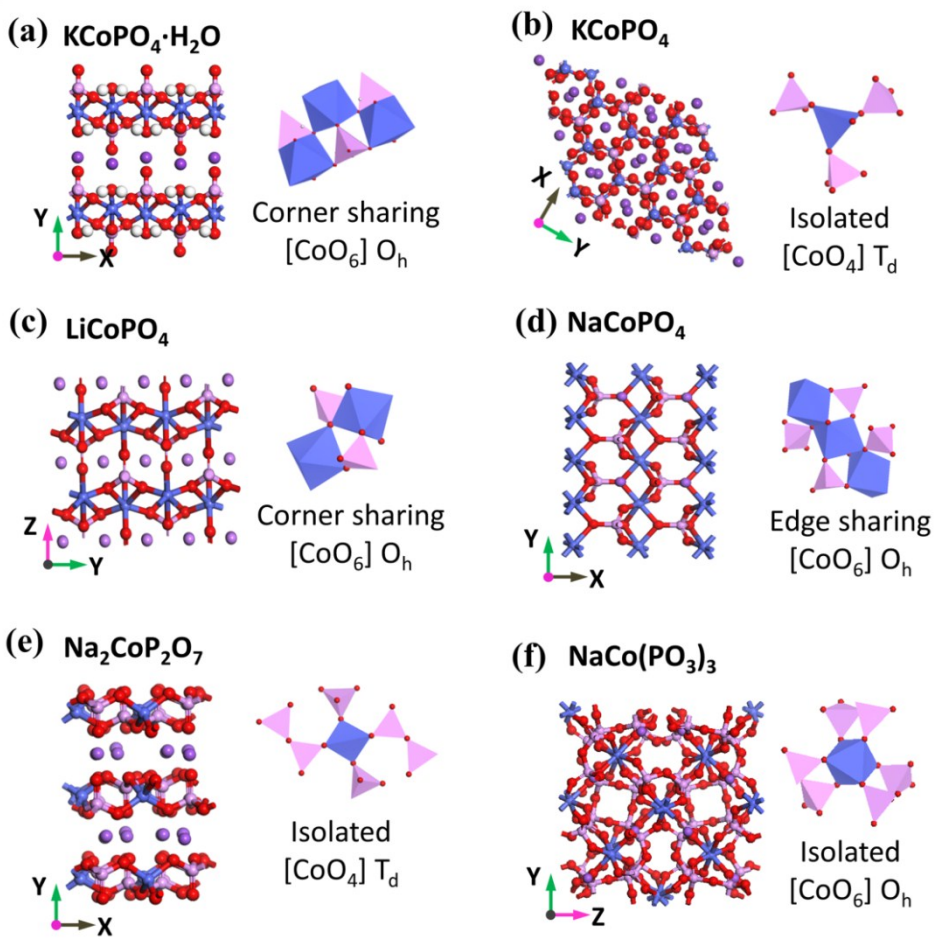

Fig. S2 Crystal structures of phosphate/pyrophosphate/metaphosphate-containing compounds with various cobalt (II) geometries including octahedral (Oh), tetrahedral (Td) and trigonal bipyramidal (TBP). The inset shows the local environment around the Co subunit (blue).

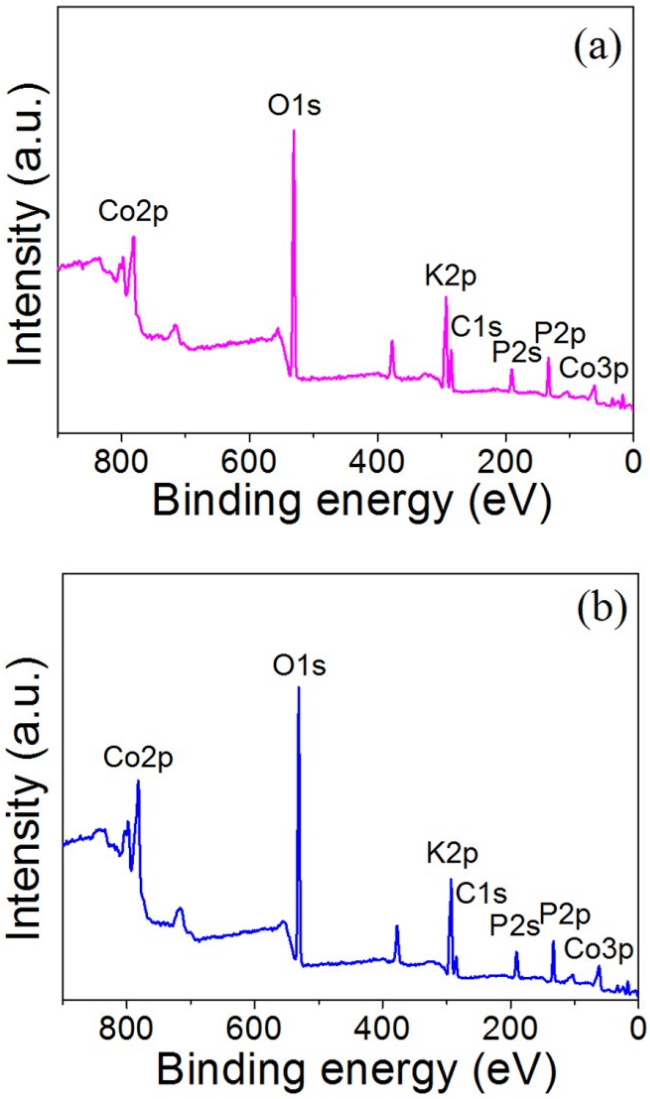

Fig. S3. Overall XPS spectra of the as-prepared (a) $KCoPO_4 \cdot H_2O$, and (b) $KCoPO_4$.

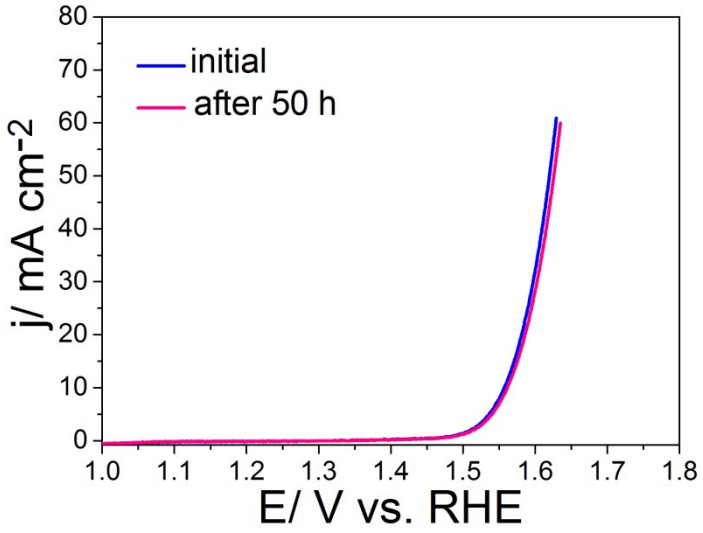

Fig. S4 LSV curve repeated after 50h test for $KCoPO_4$.

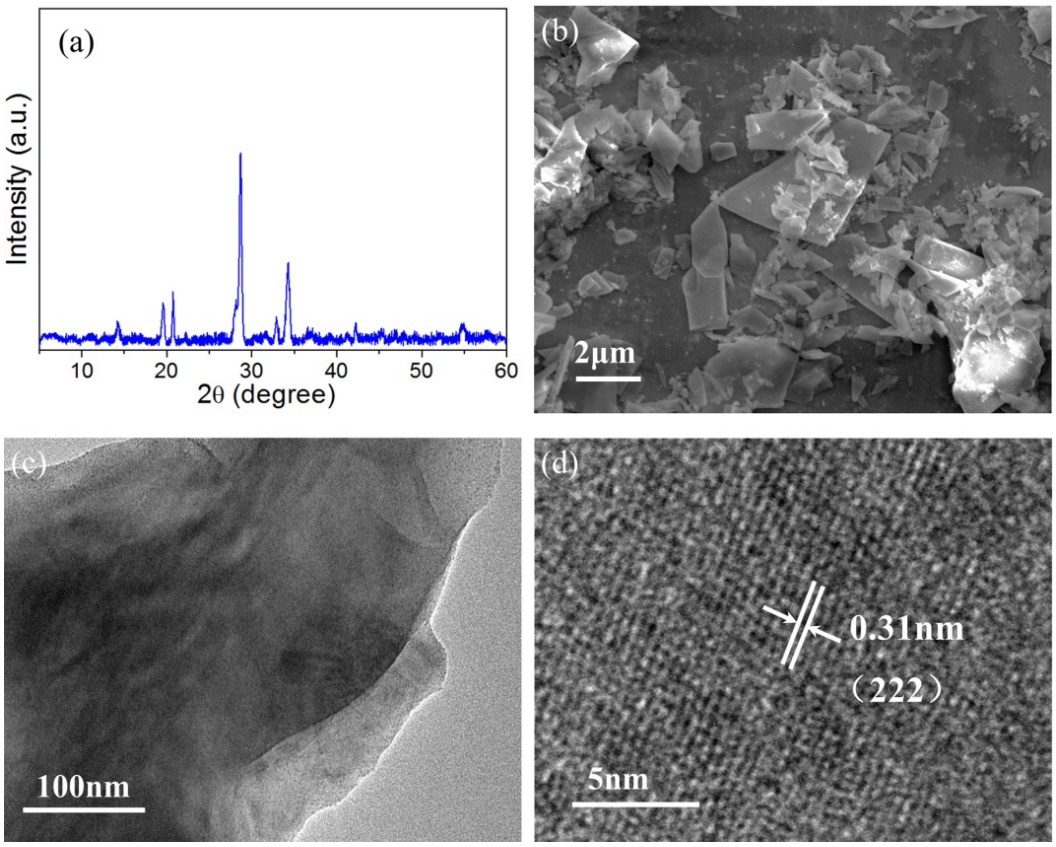

Fig. S5 Structural characterizations of $KCoPO_4$ after the chronopotentiometry process. (a) XRD pattern, (b) SEM image, (c) TEM and HRTEM image.

Table S1. Fractional atomic coordinates for $KCoPO_4 \cdot H_2O$.

	x	y	z
H3	0.791910446	6.753781256	0.785989366
O4	1.232976618	1.101077321	1.442646563
K0	0	4.523386189	3.390965417
Co1	0	8.253984906	2.855622607
P2	0	1.789777434	0.759719193
O5	0	1.515743558	4.086261412
O6	0	3.280429984	1.021655982

Table S2. Fractional atomic coordinates for $KCoPO_4$.

	x	y	z
K0	-4.374973668	7.714302405	4.171254269
K1	-0.565032886	5.382062866	4.225838932
K2	-4.821926674	13.20606404	8.529327648
Co6	-6.20944342	10.8025184	2.595405653
Co7	-7.613667315	13.47752223	5.776165078
Co8	-1.698224711	8.255533953	1.497976989
Co9	-2.997098816	10.89944522	5.842207963
P10	-3.083113463	5.454512398	1.679079065
P11	-7.665382872	13.58519586	2.415834148
P12	-1.668277872	8.159163762	6.864655112
P13	-3.071069658	10.98031935	2.495403112
O14	-2.823724767	5.418956282	0.184367868
O15	-6.47674418	12.0578781	6.654946206
O16	-1.648942303	4.03344564	6.40898796
O17	-7.134713134	13.81044269	3.842060138
O18	-0.197626519	2.014663114	6.664096183
O19	-4.79312978	10.19811979	6.375250237
O20	-2.662272756	7.153225642	6.246338123
O21	-6.746364259	14.33562465	1.437107254
O22	-2.113577204	6.461135755	2.329512049
O23	-4.430083843	11.43619505	1.921992948
O24	-2.988198327	9.444072846	2.474782603
O25	-2.1179682	8.540745131	8.283312892
O26	-2.923979328	11.50392173	3.931333025
O27	-1.629013647	9.437538626	6.007687479
O28	-0.259264875	7.538145755	6.896511659
O29	-1.924402107	11.5559376	1.648022064
K3	0	0	4.32261921
K4	0	10.74411141	4.009722687
K5	0	10.74411141	8.367098254

Table S3. OER activities of some recently reported transition-metal phosphate based electrocatalysts in alkaline aqueous electrolyte in terms of the overpotential to achieve a current density of 10 mA cm^{-2}.

Materials	Overpotential (mV)	Electrolyte	Tafel slope (mV dec^{-1})	Stability (h)	Reference
$KCoPO_4$	319	1.0 M KOH	61.8	50	This work
$KCoPO_4 \cdot H_2O$	387	1.0 M KOH	66.2	10	This work
CoHPi nanoflakes	314	1.0 M KOH	31	6.7	10
$Co_3(PO_4)_2$/RGO	405	1.0 M KOH	75	3	11
$Co_3(PO_4)_2$@N-C	317	1.0 M KOH	62	8	12
$NaCo(PO_3)_3$	340	1.0 M KOH	76	12	13
NiCoP/C	330	1.0 M KOH	96	10	14
CoPi-HSNPC-800	320	1.0M KOH	85	20	15

References

[1] X. Lu, C. Zhao, Nat. Commun. 2015, 6, 6616.

[2] M.D. Segall, P.J.D. Lindan, M.J. Probert, C.J. Pickard, P.J. Hasnip, S.J. Clark, M.C. Payne, J. Phys.: Condens. Matter. 14 (2002) 2717-2744.

[3] P. Hohenberg, W. Kohn, Phys. Rev. 136 (1964) B864-B871.

[4] W. Kohn, L.J. Sham, Phys. Rev. 140 (1965) A1133-A1138.

[5] V.I. Anisimov, F. Lichtenstein, A.I. Lichtenstein, J. Phys.: Condens. Matter. 9 (1997) 767-808.

[6] V.I. Anisimov, J. Zaanen, O.K. Andersen, Phys. Rev. B 44 (1991) 943-954.

[7] X. Fu, B. Warot-Fonrose, R. Arras, D. Demaille, M. Eddrief, V. Etgens, V. Serin, Appl. Phys. Lett. 107 (2015) 062402-062406.

[8] P.E. Blöchl, Phys. Rev. B 50(1994) 17953-17979.

[9] D. Vanderbilt, Phys. Rev. B 41 (1990) 7892-7895.

[10] J. Wang, H.C. Zeng, ACS Appl. Mater. Interfaces 10 (2018) 6288-6298.

[11] Y. Zhan, S. Yang, M. Lu, Z. Liu, J.Y. Lee, Electrochimica Acta 227 (2017) 310-316.

[12] C.Z. Yuan, Y.F. Jiang, Z. Wang, X. Xie, Z.K. Yang, A.B. Yousaf, A.W. Xu, J. Mater. Chem. A 4 (2016) 8155-8160.

[13] R. Gond, D.K. Singh, M. Eswaramoorthy, P. Barpanda, Angew. Chem. 131 (2019) 8418-8423.

[14] P.L. He, X.Y. Yu, X.W.D. Lou, Angew. Chem. 129 (2017) 1-5.

[15] L. Chen, J.T. Ren, Y.S. Wang, W.W. Tian, L.J. Gao, Z.Y. Yuan, ACS Sustainable Chem. Eng. 7 (2019) 13559−13568.